

MSL

Boron Carbide-Carbon Composites and Composites for Cryogenic Applications

by

H. Sheinberg

A. Boron Carbide-Carbon Composites

1. Introduction

Because of its neutronic properties, high hardness, and high melting temperature, boron carbide (B_4C) is widely used at the Los Alamos Scientific Laboratory. However because of its hardness and mode of manufacture, it is expensive to finish machine to tight dimensional specifications. For some neutronic applications, a density considerably below the theoretical 2.52 Mg/m^3 was acceptable, and this relaxation in density specification permitted addition of carbon as a second phase to reduce machining costs.

We conducted an experimental program to prepare 50.8-mm-diam by 34.8-mm-thick cylinders of B_4C and B_4C -C composites with concentrations of carbon varying from 5.5 to 30 volume percent. Additionally we used three forms of carbon, natural flake graphite, synthetic graphite flour, and a fine furnace black as the source of the second phase.

We determined the sound velocity, compressive strength, coefficient of thermal expansion, electrical resistivity, and microstructure as functions of composition.

2. Raw Materials

The B_4C powder used in these experiments was a nominal 6.5- μm average size powder whose structure is shown in Figure 1. Also shown are the structures of the natural flake graphite, the synthetic graphite flour, and the furnace black.

DISTRIBUTION OF THIS DOCUMENT IS UNLIMITED



B₄C, 250X



Flake Graphite, 100X



Graphite Flour 100X



Carbon Black, 500X

Figure 1 - Structure of Raw Materials.

3. Fabrication

We weighed the raw materials to 0.01 g and blended them in glass bottles equipped with 3-mm-diam aluminum agitator wires. The blended powders were leveled in graphite die assemblies, cold pressed at ~ 28 MPa, and then conventionally hot pressed at $\sim 2200^\circ\text{C}$ and at pressures ranging from 2500 to 4000 psi (24 to 28 MPa) to $98.7 \pm 0.3\%$ of theoretical density. We assumed values of 2.52, 2.26, and 2.0 Mg/m^3 for theoretical densities of B_4C , graphite, and carbon, respectively, and used the rule of simple mixtures for calculating the theoretical density of the composites.

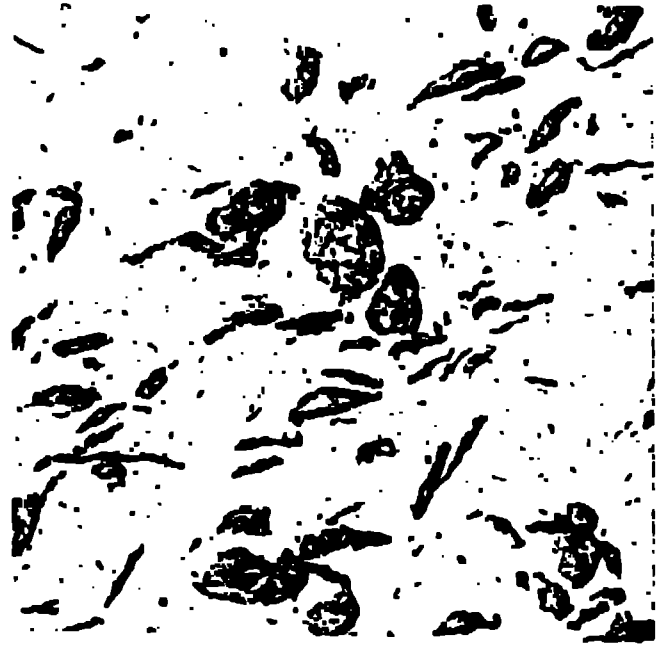
4. Structure and Properties

Most uniaxially hot-pressed refractory materials exhibit some degree of structural anisotropy. We examined the structure of these materials by metallography both parallel and perpendicular to the direction of pressing and verified anisotropy in this composite. Figures 2 and 3 show, as expected, increased anisotropy with increased volume concentration of flake graphite. The orientation of the flake graphite particles is marked in the direction normal to the pressing direction. As Figure 4 shows, structural anisotropy is decreased when synthetic graphite is substituted for flake graphite, and the structure is relatively uniform when the fine furnace black is employed. This observation is valid even though x-ray diffraction on the hot pressed material indicated that $\sim 90\%$ of the carbon initially present was converted to crystalline graphite during hot pressing and cooldown. It is postulated that the B_4C dissolves excess carbon during the hot pressing but the excess is precipitated as graphite during hot pressing and cooldown.

Chords were cut from the hot pressed cylinders to leave a specimen of equal width and thickness; opposite sides were ground flat and parallel. The sound speed was measured in both directions, and values of longitudinal and



B₄C - 8.8 vol % C, normal to pressing direction



B₄C - 8.8 vol % C, parallel to pressing direction

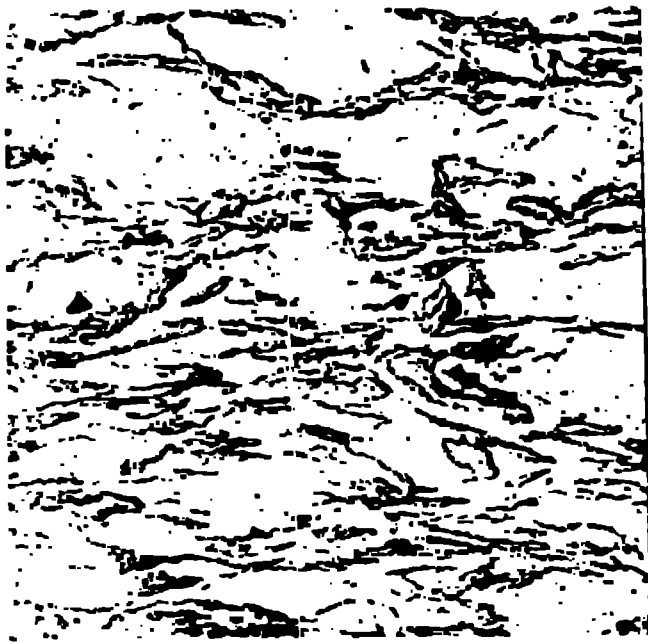


B₄C - 20 vol % C, normal to pressing direction



B₄C - 20 vol % C, parallel to pressing direction

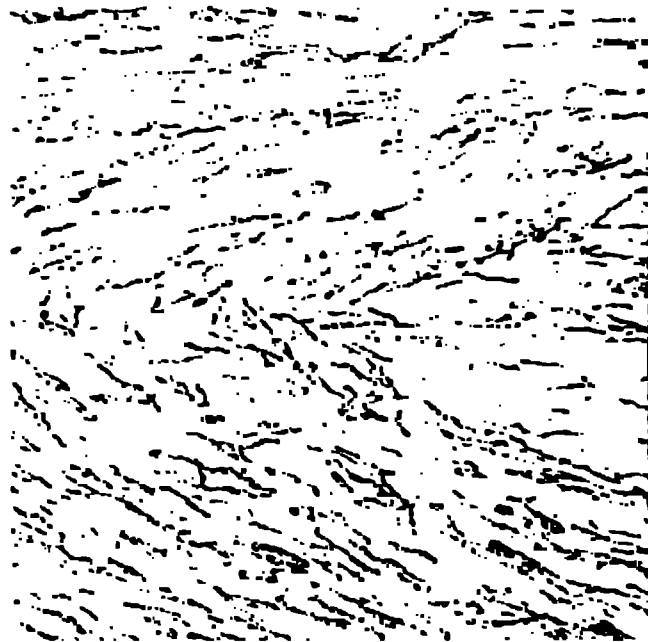
Figure 2 - Structural Anisotropy of B₄C - 8.8 and 20 vol % Flake Graphite, 100X.



B_4C - 25 vol % C, normal to pressing direction



B_4C - 25 vol % C, parallel to pressing direction

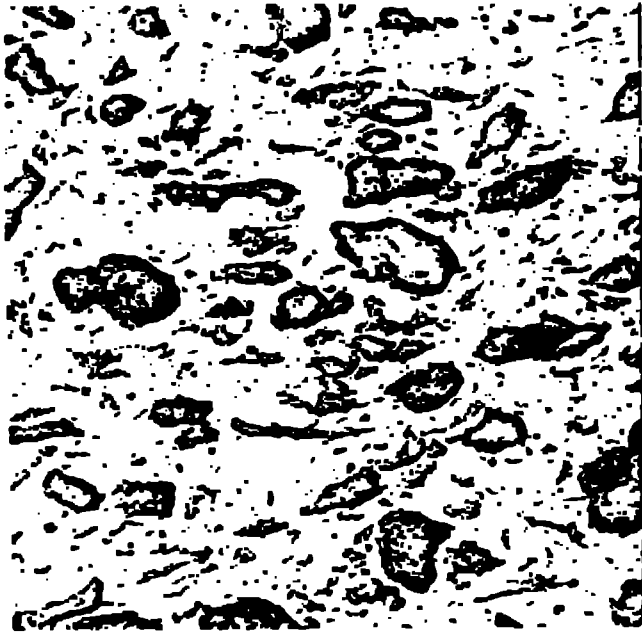


B_4C - 30 vol % C, normal to pressing direction

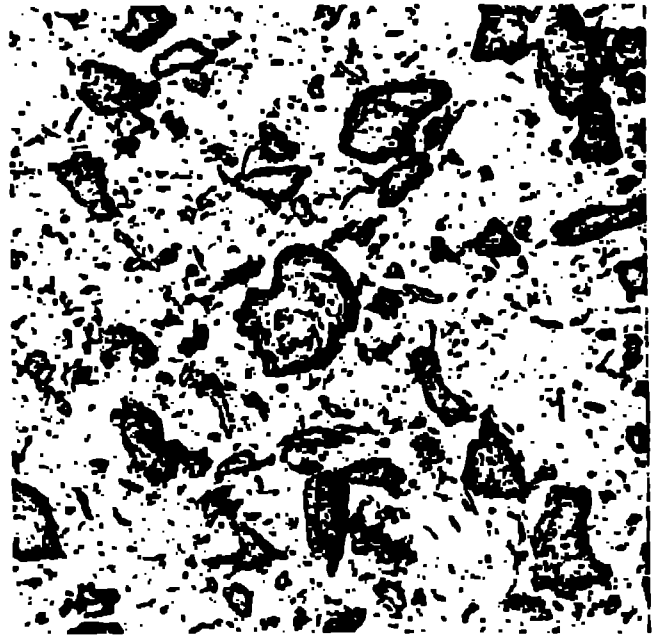


B_4C - 30 vol % C, parallel to pressing direction

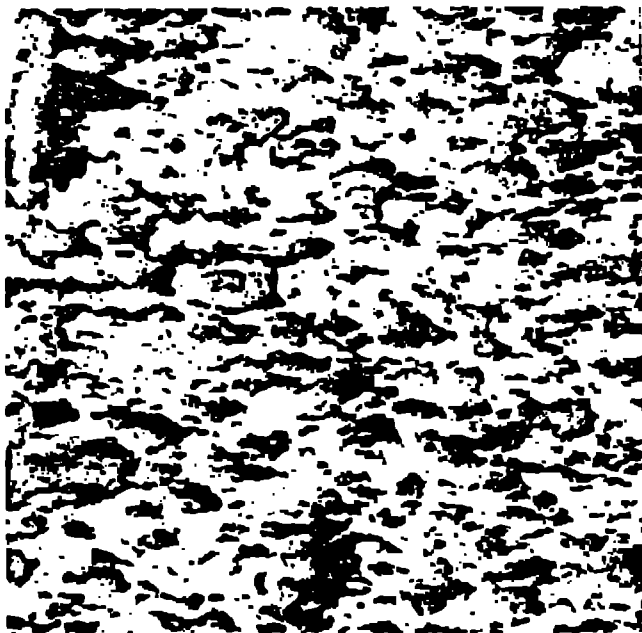
Figure 3 - Structural Anisotropy of B_4C - 25 and 30 vol % Flake Graphite, 100X.



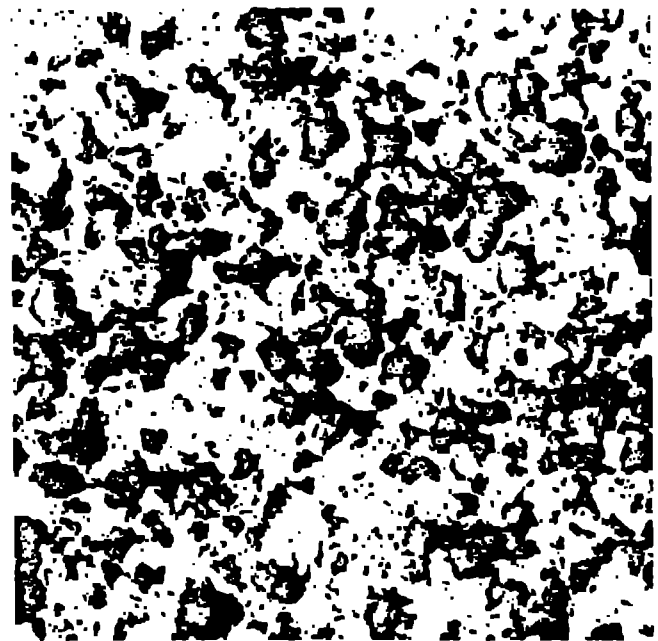
B₄C - 30 vol % Synthetic Graphite, normal to pressing direction



B₄C - 30 vol % Synthetic Graphite, parallel to pressing direction



B₄C - 30 vol % Furnace Black, normal to pressing direction



B₄C - 30 vol % Synthetic Graphite, parallel to pressing direction

Figure 4 - Structure of B₄C - 30 vol % C made using Synthetic Graphite Flour and Furnace Black, 100X.

shear waves (as defined by Figure 5) were determined. The data on B_4C and B_4C plus flake graphite plotted in Figure 6 clearly indicate the increased anisotropy with increased flake graphite. To preserve graph clarity, the sound speed data obtained from cylinders fabricated with 30 vol % graphite flour and furnace black (Thermax) are recorded in Table I, together with data from equivalent flake graphite additions, and compared. The sound speed data correlate with the metallography.

Compression specimens, 5 mm in diameter by 15 mm long, also were machined from the hot pressed cylinders, both parallel and perpendicular to the direction of pressing. Test results are plotted in Figure 7.

We used a differential scanning calorimeter to measure heat capacities from 343 to 743°K on three B_4C -C specimens made with 20 and 30 vol % carbon. The data in Table II indicate considerable differences in heat capacity among the 30 vol % pressings in which the carbon sources were synthetic graphite flour and natural flake graphite, and as great a difference between the pressings made with 20 and with 30 vol % flake graphite.

Table II - Heat Capacity of Boron Carbide-Graphite Composites

T(°K)	C_p (cal/g)		
	R16B	R15	R13A
	30 vol % Graphite Flour	30 vol % Flake Graphite	20 vol % Flake Graphite
343	0.253	0.265	0.275
373	0.277	0.290	0.287
423	0.309	0.304	0.317
473	0.336	0.333	0.355
573	0.385	0.397	0.423
673	0.463	0.415	0.443
753	0.452	0.445	0.469

$$R16B \quad C_p = - 0.087 + 1.2 \times 10^{-3} T - 6.23 \times 10^{-7} T^2.$$

$$R15 \quad C_p = - 0.0051 + 9.47 \times 10^{-4} T - 4.66 \times 10^{-7} T^2.$$

$$R13A \quad C_p = - 0.089 + 1.29 \times 10^{-3} T - 7.29 \times 10^{-7} T^2.$$

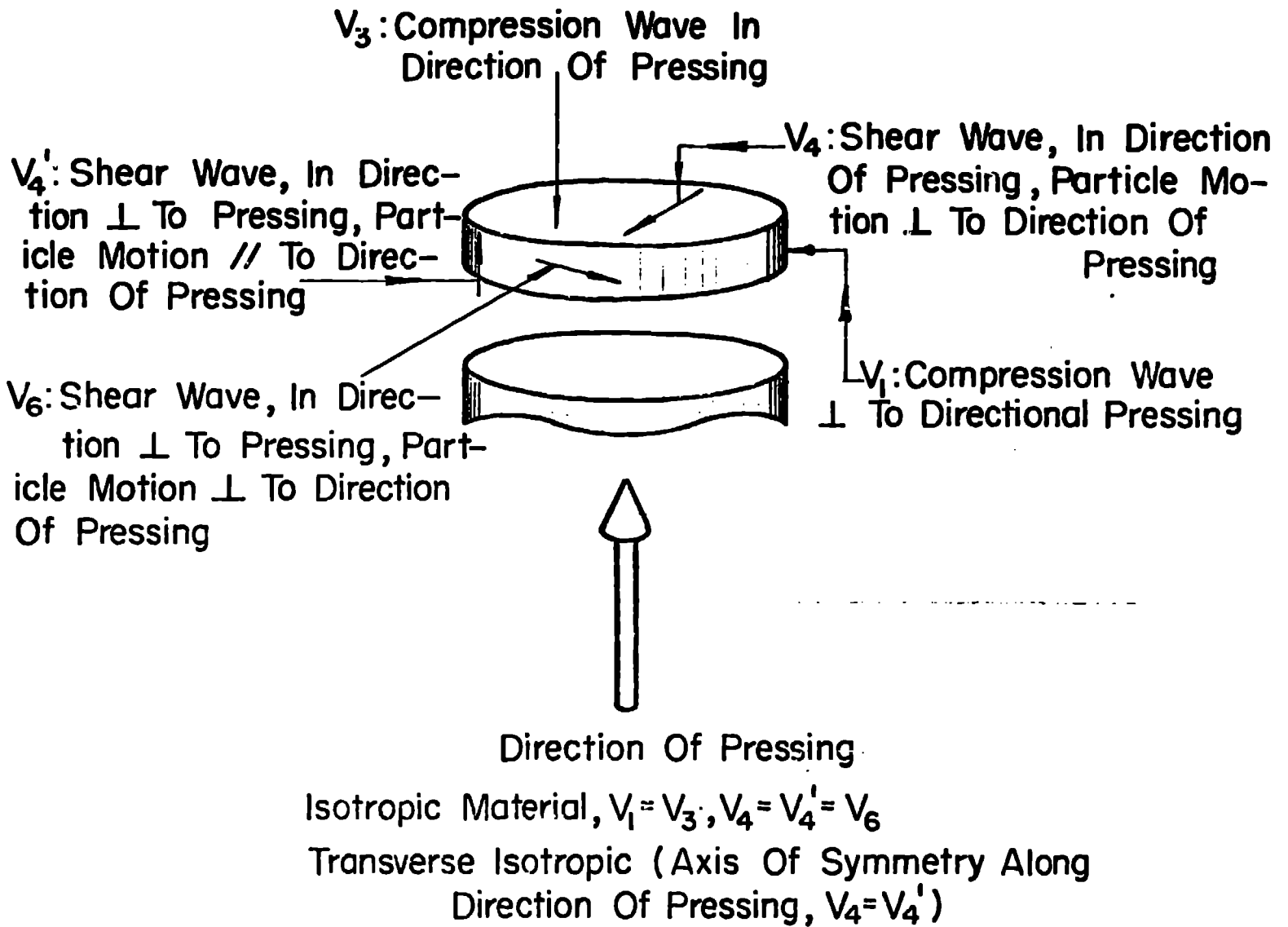


Figure 5 - Longitudinal and Shear Waves.

Fig. 6 , Sound Speed vs Volume Percent Graphite In B_4C-C Composite

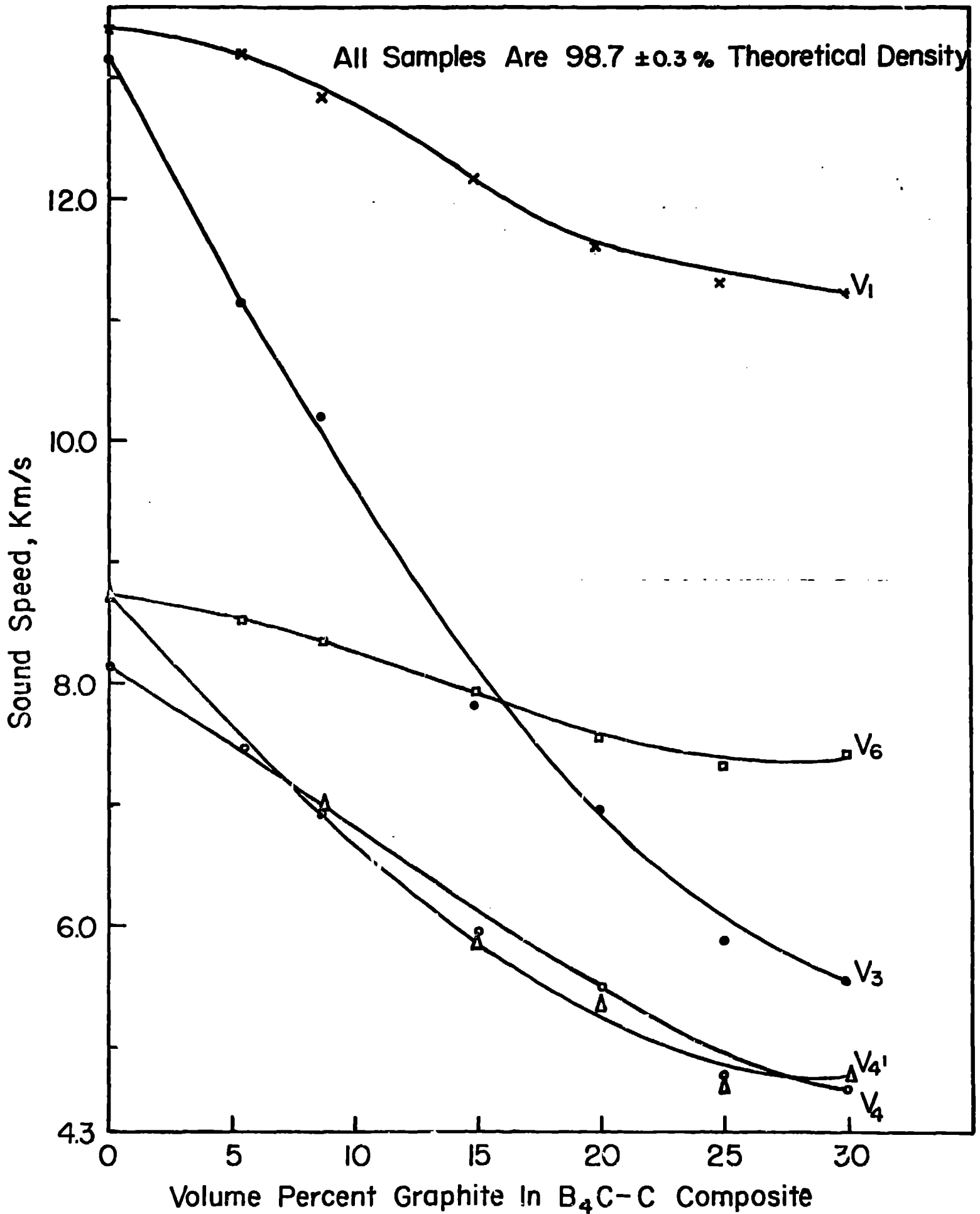


Table I - Sound Speed of Boron Carbide and Boron Carbide-Carbon Composites

<u>Sample Number</u>	<u>Composition</u>	<u>Density % Theoretical</u>	<u>V₁</u>	<u>V₃</u>	<u>V₄</u>	<u>V₄'</u>	<u>V₆</u>
R7	B ₄ C - 8.8% Graphite	96.1	12.80	10.92	7.17	7.64	8.07
R8	B ₄ C -	98.8	13.40	13.22	8.15	8.73	8.73
R9	B ₄ C - 8.8% NF Graphite	99.0	12.84	10.16	6.99	6.99	8.32
R10	B ₄ C - 5.5% NF Graphite	99.0	13.21	11.16	7.45	7.42	8.51
R12	B ₄ C - 15.0% NF Graphite	98.9	12.18	7.84	5.94	5.90	7.92
R13A	B ₄ C - 20.0% NF Graphite	98.7	11.63	6.96	5.48	5.36	7.55
R14	B ₄ C - 25.0% NF Graphite	98.6	11.32	5.89	4.77	4.71	7.31
R15	B ₄ C - 30.0% NF Graphite	98.5	11.22	5.53	4.66	4.75	7.42
R16A	B ₄ C - 30.0% Graphite	98.7	10.66	8.74	5.86	5.86	6.60
R2A	B ₄ C - 30.0% Thermax	98.1	9.55	6.63	4.85	4.88	6.01

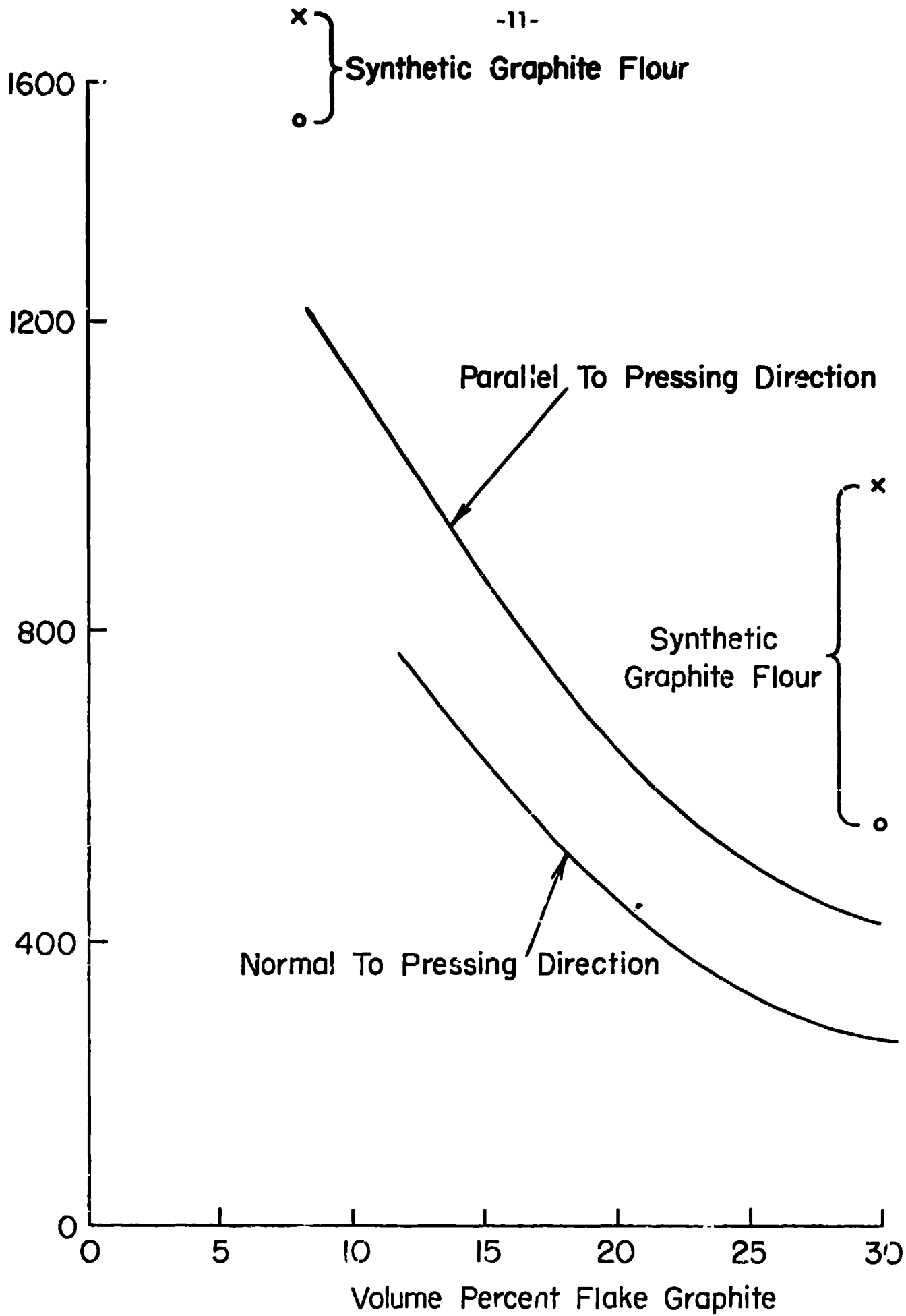


Figure 7. Compressive Strength of Boron Carbide-Carbon Composites.

B. Boron-Carbon Composites

1. Introduction

Normal boron carbide pressed to 95% of theoretical density was urgently required for use as a neutron absorber, safety rods, and control rod assemblies for a reactor. The B_4C was 11.43 ± 0.25 and 29.21 ± 0.25 mm in diameter by $522.48 \begin{smallmatrix} + 0 \\ - 0.13 \end{smallmatrix}$ mm long, and the number of pieces making up the 522.48-mm length was immaterial. Seven of the larger diameter and three of the smaller diameter 522-mm-long rods were required.

We suggested as an alternate material and alternate fabrication processes, an enriched boron (^{10}B)-carbon composite made by (1) isostatically pressing a mixture of ^{10}B and carbonaceous powders bonded with furfuryl alcohol and then curing and baking the pressings as described in earlier work*, or by (2) the very simplest of processes, isostatically pressing a blended mixture of ^{10}B and flake graphite powders. We believed that we should be able to make such a composite that would have the same concentration of ^{10}B atoms/cm³ as that in 95% dense natural B_4C . The alternate material was accepted with the provision that it have a minimum ^{10}B concentration of 2.18×10^{22} atoms/cm³ (concentration of ^{10}B in 100% B_4C).

2. Raw Materials

We screened graphite flour and a furnace black through a 325-mesh screen after oven drying them. The enriched boron powder lot was 94.6 atom percent ^{10}B and 5.4 atom percent ^{11}B . The structure and size of this powder are shown in Figure 8. A partially polymerized furfuryl alcohol catalyzed with 4 g of maleic anhydride/100 cm³ of alcohol was used as a binder.

For the pressings of ^{10}B and flake graphite, we used Union Carbide

*U.S. Patent No. 3,126,625 "Graphite Production Utilizing Uranyl Nitrate Hexahydrate Catalyst," by H. Sheinberg, D. H. Schell, and J. R. Armstrong.



B-94.6, 100X



B-94.6, 250X

Figure 8 - Size and Structure of Enriched Boron Powder.

Corporation grade SP-1 screened -200 mesh, Superior Graphite Company grade Superflake SSG-59, and Joseph Dixon Crucible Company grade 635 flake graphite powders.

3. Fabrication Feasibility

We used a composition of 17.69 wt% ^{10}B , 70.00 wt% graphite flour, and 12.32 wt% Thermax. To 100-g portions of this blend, we added 25, 30, 33, and 35 g of catalyzed Varcum, then hand mixed the wetted powder and passed it three times through a miniature meat grinder. The thoroughly mixed material was passed through a 20-mesh screen and tamped into 38-mm-i.d. polyvinyl alcohol sacks which were evacuated and pressed at 345 MPa. We cured the pressings in a 63-h curing cycle from room temperature to 250°C and then baked them under vacuum to 850°C in a 48-h cycle.

We then machined the very abrasive baked pieces with diamond tooling. Geometric densities (disappointingly low) were as follows.

<u>Run No.</u>	<u>Wt. Varcum</u>	<u>Density (Mg/m³)</u>
PL-1	25	1.63
-2	30	1.67
-3	33	1.71
-4	35	1.73

We pressed blends of 21.00 wt ^{10}B - 79 wt flake graphite isostatically at 345 MPa. These pressings were machined very easily into right cylinders (with sharp corners) by conventional carbide tooling. Pressed densities were as follows:

<u>Flake Graphite</u>	<u>Density (% of theoretical)</u>	<u>^{10}B (atoms $^{10}\text{B}/\text{cm}^3$) Concentration</u>
SP-1	89.4	2.34×10^{22}
Superflake	91.7	2.39×10^{22}
Dixon	90.5	2.36×10^{22}

These very high as-pressed densities, coupled with the certainty of composition, and the very high ^{10}B atomic concentration make this a very simple, economical, and fast mode of fabrication. However, note that these pressings are not very strong; they are strong enough for machining, but would have to be handled carefully during assembly, and it is possible that reactor operating conditions could cause some powdering of the pressings.

On the other hand, the furfuryl alcohol bonded and baked pressings were quite strong and hard, so we decided to pursue this process for fabricating the enriched boron components even though it is more costly and time-consuming and, because of the uncertainty of the residual carbon from polymerization of the alcohol, the atomic concentration of ^{10}B must be determined by chemical analysis.

We then made 1800-g blends using the ^{10}B to which we added 33 wt% alcohol. We processed these mixtures as indicated previously, but used a 4-qt Patterson-Kelly twin shell blender equipped with agitator and liquid addition insert for dry blending and alcohol addition, and used a larger Hobart meat grinder for homogenizing the wet blend. The powder was screened and tamped into 34.9-mm-diam by 150-mm-long or 22.2-mm-diam by 101-mm-long plastic sacks and pressed at 345 MPa. Most of the pressings broke into two pieces.

After being cured and baked, the pieces were machined to dimensional specifications with diamond tooling.

4. Properties of Composite

The densities of the large diameter stacks ranged from 1.75 to 1.77 Mg/m³ and those of the small diameter stacks from only 1.69 to 1.70 Mg/m³. The boron content (reported and calculated as ¹⁰B) analyzed from 21.6 to 21.9 wt%. From these analyses and measured geometric densities, the ¹⁰B concentrations reported in Table III were calculated.

Table III - Properties of Boron-Carbon Composites

<u>Stack No.</u>	<u>Density (Mg/m³)</u>	<u>Blend No.</u>	<u>¹⁰B Concentration 10²² atoms/cm³</u>
1	1.76	5	2.32
2	1.77	5 and 6	2.31
3	1.76	5	2.32
4	1.76	6	2.28
5	1.76	6	2.28
6	1.75	7	2.27
7	1.76	7	2.28
1A	1.70	8	2.02
2A	1.69	8	2.01
3A	1.69	8	2.01

Although some of the pressings broke into two or three pieces lengthwise on unloading, none of the pieces fractured during machining and we obtained sharp corners on the machined cylinders. Although this ¹⁰B-C composite is not as strong and homogeneous as hot-pressed B₄C, the items were fabricated at probably less than one tenth the labor cost that would have been required to hot press and grind the B₄C. Note that we used expensive ¹⁰B powder, rather than the relatively inexpensive (\$50.00/kg) B₄C.

We believe the lower density of the small-diameter pieces was caused by a lower tamped density in the small-diameter sacks. The atomic concentration

of ^{10}B in these small-diameter pressings was slightly lower than specified but essentially the same as that in the 95% dense B_4C originally specified. The concentration of ^{10}B in the larger diameter control rods was higher than required.

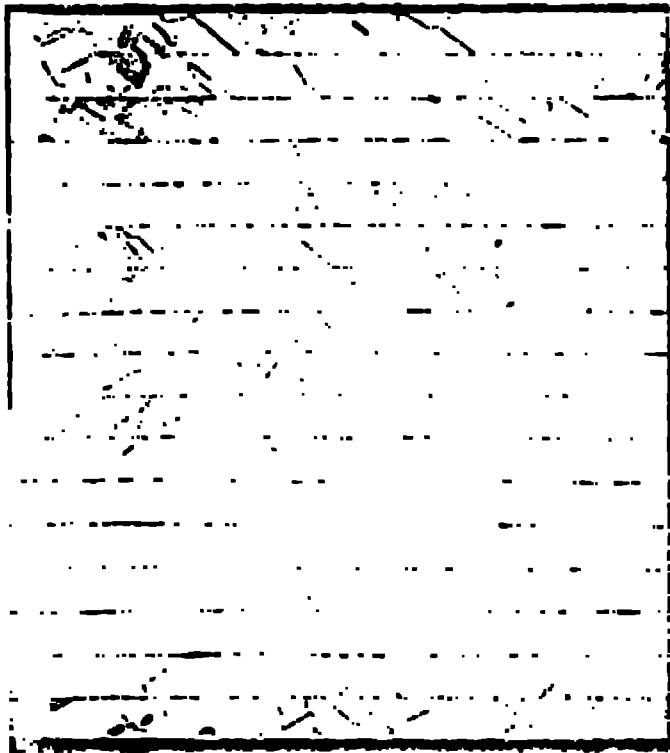
Although we didn't use the simple cold-pressing fabrication process, we did demonstrate that we could easily make machinable cylinders of flake graphite and ^{10}B with ^{10}B concentrations considerably higher than that in 100% dense normal B_4C . We accomplished this without the luxury of having time to vary particle size and/or size distribution of either the ^{10}B or the graphite to maximize pressed density.

Probably with more trial runs in which we would vary the binder content in smaller graduations, we could make crack-free, slightly higher density ^{10}B -C composites; close control of the particle size of the ^{10}B powder should also promote a slight increase in density.

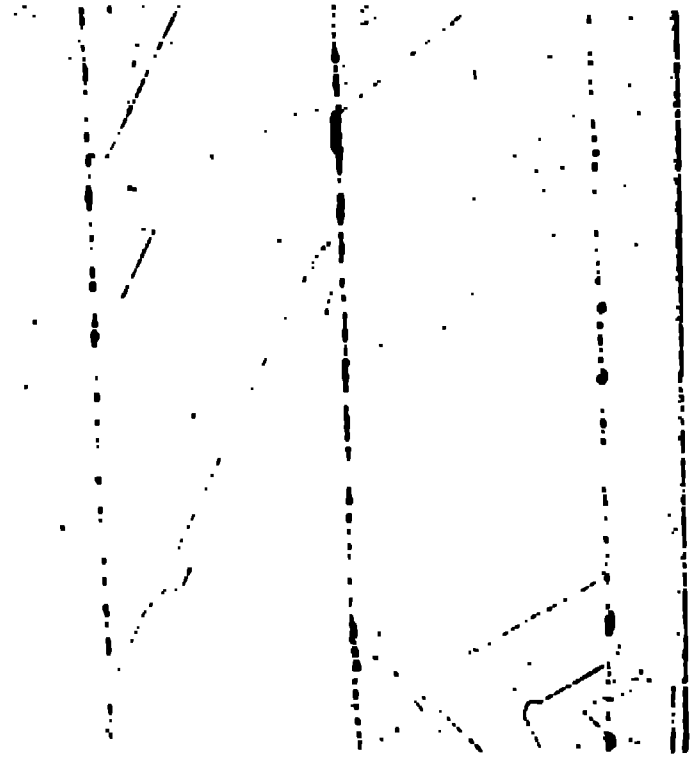
C. Composites for Cryogenic Application

For use in cryogenic refrigeration, in an effort to enhance adiabatic stability, we fabricated copper disks containing gadolinium oxide (Gd_2O_3) or gadolinium aluminum oxide (GdAlO_3). We initially hot pressed seventeen layers of 0.41-mm-thick high-purity copper sheet, 25.4 mm square, in a graphite die at 1000 psi (6.9 MPa) and 800°C for 1 h to yield a 38-mm-diam by 5.83-mm-thick disk. The structure of the pressed disk is shown in Figure 9. The black areas in the photomicrograph are voids at the interfaces, but it is apparent that adjacent layers were well bonded and that many of the large copper grains crossed many of the initial layer interfaces.

In a similar manner we hot pressed a seventeen-layer stack of copper squares, each coated with a layer of Gd_2O_3 on one surface so that the overall Gd_2O_3 content of the stack was ~2.3 wt%. We hot pressed another assembly which utilized



17X



100X

Figure 9 - Hot-pressed layers of copper.

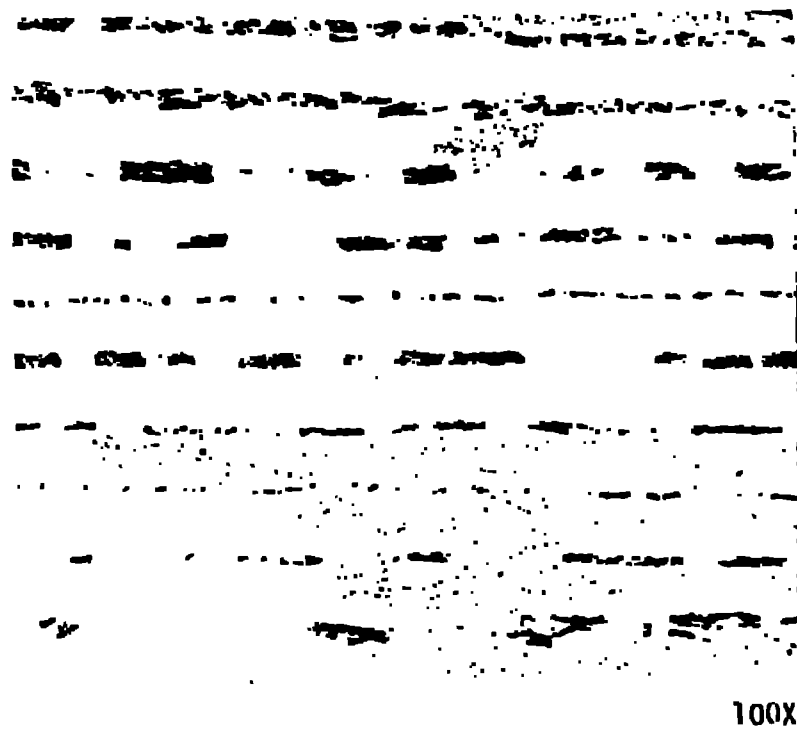


Figure 10 - Structure of copper-2.3 wt% gadolinium oxide.

a mixture of copper powder mixed with the oxide powder to provide a concentration of ~ 3 wt% Gd_2O_3 - 3 wt% Cu. The structure of this pressing is shown in Figure 10; the dark discontinuous areas are gadolinium oxide. Again, copper grains extending through several layers give ample evidence of excellent layer-to-layer bonding.

Similar pressings were made with 3.7, 3.8, 2.6, and 7.3 wt% Gd_2O_3 and 11.2 wt% $GdAlO_3$. The specific heat content of these copper assemblies was 1 - 2 orders of magnitude higher than that of the copper without the oxide.

A laboratory experiment required a system that used adiabatic demagnetization of cerium thiocyanate-oxyphosphate, $Ce(SCN)_3(OP\phi)_4$, to pump heat from a low-temperature thermal reservoir for experiments at approximately 10 mK which require handling large heat loads. A principal component of this system is a cylinder of 35 vol % copper - 65 vol % $Ce(SCN)_3(OP\phi)_4$, 44.5 mm in diameter by 44.5 mm long, with copper thermal leads in the cylinder and projecting from both ends.

We crushed the $Ce(SCN)_3(OP\phi)_4$ salt, screened it to -45 +200 mesh, and blended this powder with a nominal 1- μ m average particle size copper powder that had been freshly reduced in H_2 and screened through a 325-mesh screen. The powders were blended in a glass container with aluminum agitator wires.

We inserted a punch with sixteen 1.82-mm-diam holes through its length (shown in Figure 11) into the bottom of a 44.5-mm-i.d. hardened steel die. We then inserted eight twisted, 0.41-mm-diam, etched, 99.999% pure copper wires through each hole so that they extended approximately 109 mm above the punch face into the die cavity. We gently vibrated the blended powder into the die cavity around the wires and leveled it at a height that left the ends of the wires visible. The top 42.8-mm-long punch was positioned in the die with the 0.51-mm-diam holes facing the powder and wire charge. We inserted single,

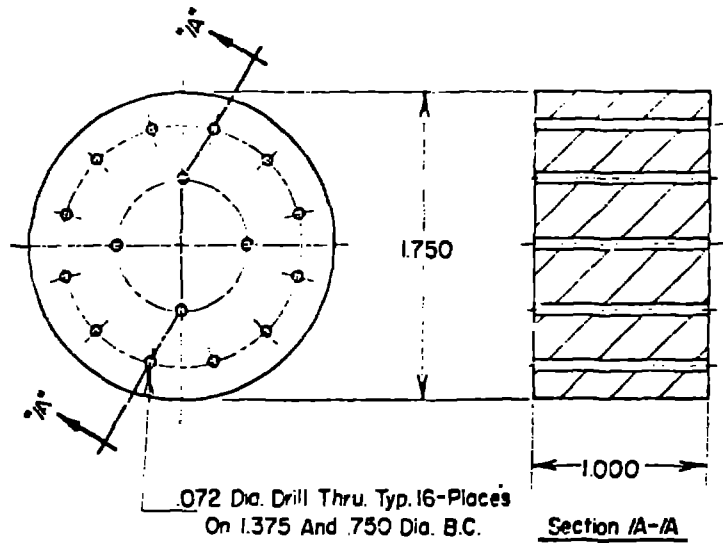
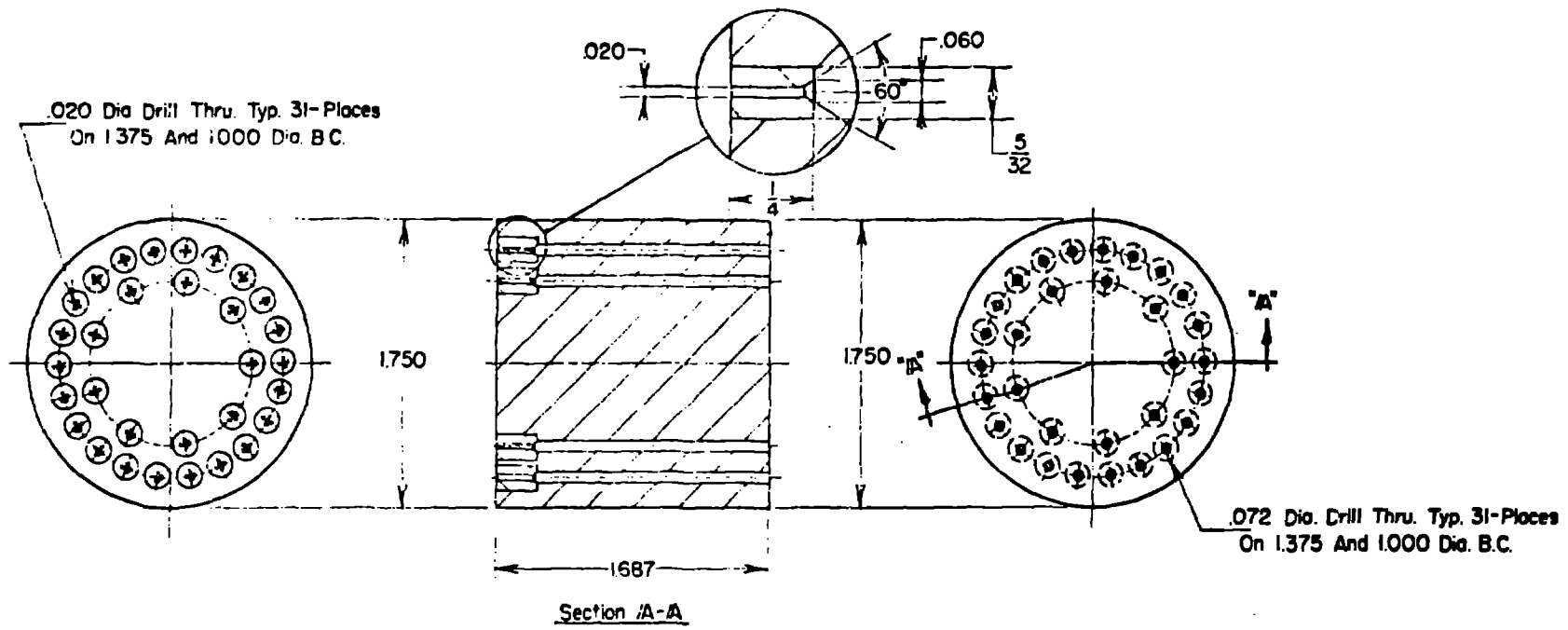


Figure 11 - Punches for Die Assembly.

0.41-mm-diam by 150-mm-long, etched copper wires into the outer twenty-one holes and pushed them through the entire 108-mm-diam column of powder so that their upper ends were flush with the top of the punch.

We slowly pressed the powder and wire charge to a maximum pressure of 345 MPa, held that pressure for 60 s, and then ejected the compacted cylinder together with the two punches. The punches were then carefully pulled off the cylinder leaving the wires projecting from both ends. The compacted assembly is shown in Figure 12.

We subsequently made a similar cylinder using gold instead of copper, and this cylinder also performed satisfactorily in a refrigeration unit, as did a similar cylinder of gold and cerium magnesium nitrate.

Acknowledgments

The author is indebted to J. Kostacopoulos and N. K. Richerson for their assistance in fabrication of the composites, to the Physical Metallurgy Section of Group CMB-6 for the metallography and compression testing, and to R. N. Rogers for the heat capacity measurements. The Graphite Section of Group CMB-6 cured and baked the furfuryl alcohol bonded specimens.

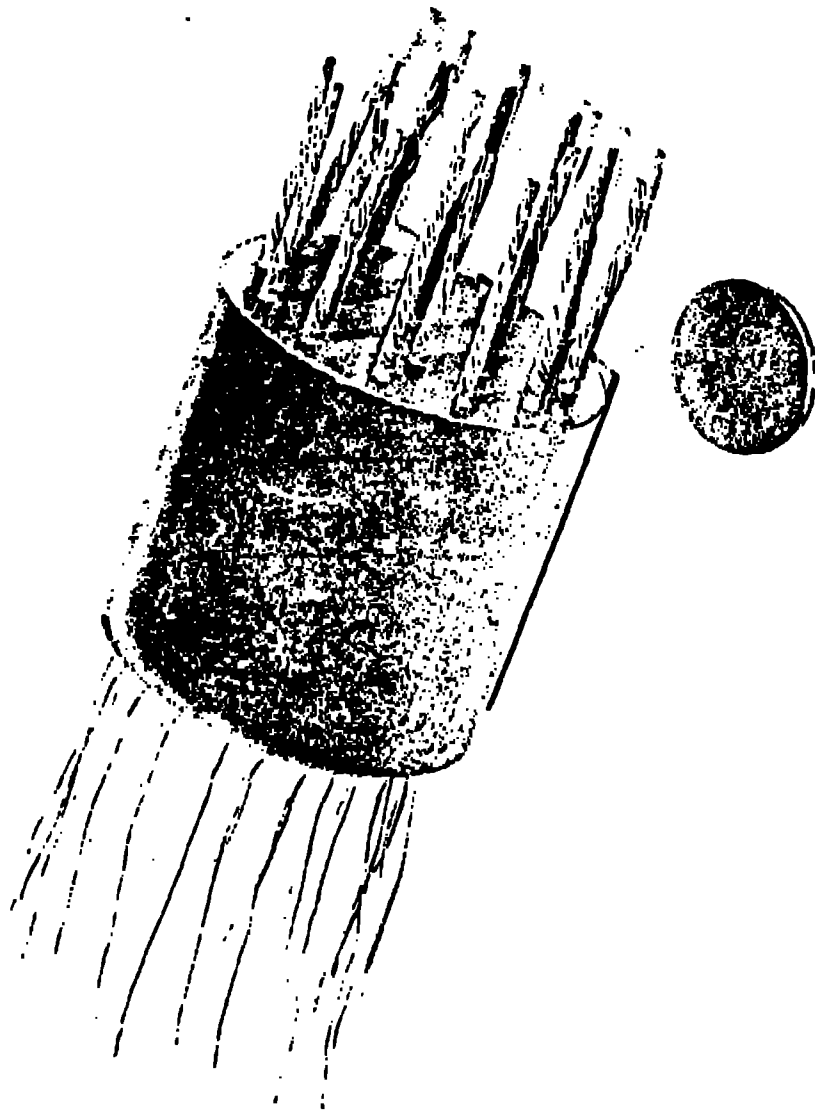


Figure 12 - Copper-Cerium Salt Demagnetization Pill.